

EDITOR

Pierfrancesco Morganti

Dermatology Unit, University of Campania “Luigi Vanvitelli”, Naples, Italy;

China Medical University, Shenyang, China;

Director of the R&D Nanoscience Centre MAVI, MAVI Sud Srl, Aprilia (Lt), Italy.

Editorial Office

MDPI

St. Alban-Anlage 66

4052 Basel, Switzerland

For citation purposes, cite each article independently as indicated below:

| |
|--|
| LastName, A.A.; LastName, B.B.; LastName, C.C. Chapter Title. In <i>Bionanotechnology to Save the Environment. Plant and Fishery's Biomass as Alternative to Petrol</i> ; Pierfrancesco Morganti, Ed.; MDPI: Basel, Switzerland, 2018; Page Range. |
|--|

ISBN 978-3-03842-692-9 (Hbk)

ISBN 978-3-03842-693-6 (PDF)

doi:10.3390/books978-3-03842-693-6

Cover image courtesy of Pierfrancesco Morganti.

© 2019 by the authors. Chapters in this volume are Open Access and distributed under the Creative Commons Attribution (CC BY 4.0) license, which allows users to download, copy and build upon published articles, as long as the author and publisher are properly credited, which ensures maximum dissemination and a wider impact of our publications.

The book taken as a whole is © 2019 MDPI under the terms and conditions of the Creative Commons license CC BY-NC-ND.

Chitin Nanofibrils-Chitosan Composite Films: Characterization and Properties

Galina Tishchenko, Pierfrancesco Morganti, Marco Stoller, Ivan Kelnar, Jana Mikešová, Jana Kovářová, Jindřich Hašek, Radomír Kužel, Miloš Netopilík, Ludmila Kaprálková, Milena Špírková, Ewa Pavlová, Eliška Chanová, Libuše Brožová, Michal Pekárek, Libor Kobera, Zdenka Sedláková and Dana Kubies

Abstract: In this research, an attempt to prepare a prototype of fully biodegradable nanocomposite films for food packaging was made by using commercial chitosan (CS) and chitin nanofibrils (CN). If food products could be packaged in these innovative films instead of paper (cellulosic) ones, the speed of deforesting in Europe will be diminished, thus improving the ecological situation and climate. In the paper, properties of the CS/CN films are described. The prototype films have been prepared from aqueous viscous CS/CN slurries by casting technique. The effect of many operating variables on morphology and properties of the nanocomposite CS/CN films such as sorption of water vapors, oxygen permeability, contact angle, mechanical stability and thermostability is analyzed and discussed. The examined variables are CN content, type of plasticizers (polyglycerols) and their content, type of metal ions such as Mg^{+2} , Ca^{+2} , Ba^{+2} and type of various additives (gelatin, lignin and monolignols) or surface modifiers (polylactides, polyglycerol polyricinoleate). Special attention was paid to the study of the effect of the storage time of the slurries on their aging and mechanical characteristics of CS/CN films.

1. Introduction

This research solves several particular problems of the global European project Bioeconomy, designed to become the basis of a new lifestyle for future generations. The goal of Bioeconomy is to create a more sustainable future, where all natural resources will be used in the most rational and efficient way for existence of a “zero waste” society. As a concrete example of Bioeconomy in action, the utilization of waste from the fishing industry can be considered. The production of chitin nanofibrils (CN) and chitosan (CS) from exoskeletons of crustaceans, which are accumulated in huge quantities in fisheries daily, improves not only the ecological situation but also creates additional sources of renewable feedstock. New products based on CS and its derivatives and based on CN have been already applied in medicine, dermatology, cosmetics, and material science.

Nature is the most skillful designer of myriad nanocomposites. Crustaceans' exoskeletons (the polysaccharide-protein-mineral nanocomposites) are typical examples [1]. The integuments of crustaceans contain the linear water-insoluble homopolymer of β -(1 \rightarrow 4)-linked *N*-acetyl-D-glucosamine (GlcNAc) in the form of nanofibrils composed mainly from α -chitin with antiparallel orientation of GlcNAc chains. Each chitin nanofibril, about 3 nm in diameter and 300 nm long [1], is formed by a bundle of 20–30 α -chitin chains interconnected with multiple hydrogen bonds and hydrophobic interactions. CN, as is well known, are nanocrystals [2–4], which reinforce the non-crystalline proteins in carapaces just as the steel reinforcement strengthens concrete panels. The surface of CN serves for proteins enveloping them perhaps as a template. Micro- and nano-crystals of calcium carbonate and phosphate are distributed chiefly between protein molecules and probably affect their mobility and spatial arrangement [1], finally enhancing their rigidity.

In material science, mainly chitosan (deacetylated chitin) has been of interest since its discovery in 1811 by Henri Braconnot. Owing to solubility in acidified water at pH 4–4.5, a lot of remarkable properties of chitosan, including its excellent film-forming ability, have been discovered and recently exploited in many applications [5]. In contrast to rigid CN, CS chains bearing protonated amine groups in glucosamine (GlcN) rings are repelled and the chains acquire flexibility. However, the hydrophobic parts of CS chains are less flexible due to intra-chain hydrogen bonds between the atom HO3 of one sugar unit and the O5 atom of the next monosaccharide in the same chain that reduces the conformational variability. The chains with block-distribution of GlcNAc rings form the micelle-like aggregates which are interconnected by almost fully deacetylated CS chains stretched by electrostatic repulsion. The molecular dynamic simulations have shown that in such aggregates, the density of chain packaging is higher than that of aggregated chains with uniformly distributed acetylated rings. These phenomena are enhanced by increasing the acetylation degree (DA) affecting the viscosity of CS solutions [6]. After evaporation of plasticizing water molecules, the dissociation of acid molecules decreases, the protonation of CS chains is suppressed, and their repulsion becomes so negligible that they come together forming homogeneous and transparent CS films. The dried flexible CS films are stable so long as they are not in contact with water, which can promote their swelling and even complete dissolution. The non-protonated CS films are stable in water at neutral pH. They are obtained when counterions and free acid molecules, which remained inside after drying the slurries, are removed from the dried films. This is usually achieved by dipping the dried CS films in the alkaline solution followed by rinsing with water and drying. For preparing chitosan films stable in aqueous solutions in a wide pH range, the CS chains must be crosslinked with covalent bonds using bifunctional agents (e.g., glutaric

dialdehyde, genipin and, etc.). Both procedures make the practical realization for production of CS films at large scale difficult.

An alternative simple method based on “physical crosslinking” of CS chains with chitin nanofibrils is described in this paper. It has been developed for preparing biodegradable water-insoluble-at-neutral-pH nanocomposite CS/CN films for use in food packaging.

2. Experimental Methods

2.1. Solid State ^{13}C CP/MAS NMR

1D solid-state NMR spectra were measured using a Bruker Avance 500 NMR spectrometer. Magic angle spinning (MAS) frequency of the sample was 10 kHz. In all cases the dried samples were placed into the ZrO_2 rotors and stored under silica-gel to prevent rehydration. Amplitude-modulated cross-polarization (CP) with duration 1 ms was used to obtain ^{13}C CP/MAS NMR spectra with 5 s recycle delay. The ^{13}C scale was calibrated with glycine as external standard (176.03 ppm—low-field carbonyl signal).

2.2. Fourier Transform Infrared Spectroscopy (FT-IR)

FT-IR spectra were recorded using a spectrophotometer Perkin-Elmer Paragon 1000PC and Attenuated total reflection technique Specac MKII Golden Gate Single Reflection ATR system with a diamond crystal; the incidence angle was 45° . The 16 scan-spectra with 4 cm^{-1} -resolution were recorded in the range of wavenumbers: $4400\text{--}450\text{ cm}^{-1}$ and evaluated using Spectrum 2.00 software. The samples were directly applied without modification to the diamond crystal and measured.

2.3. Size Exclusion Chromatography (SEC)

The commercial chitosan (Giusto Faravelli SpA, Italy) (DA = 22%) was analyzed by SEC with dual light scattering-concentration detection: a light-scattering photometer (DAWN DSP-F, Wyatt Technology Corp.) measuring at 18 angles of observation and a differential refractometer (Shodex RI 71) were the detectors. The mobile phase was the acetate buffer, 0.15 M ammonium acetate/0.2 M acetic acid buffer (pH 4.5) and chitosan solutions ($1\text{--}5\text{ mg}\cdot\text{mL}^{-1}$) were filtered through $0.2\text{-}\mu\text{m}$ pore size disposable syringe filters (Watrex) before injection. Two columns PL Aquagel OH-MIXED B was the separation system.

For studied chitosan samples, molecular weight was also determined by measuring the intrinsic viscosity $[\eta]$. The viscosity-average molecular weight M_η was calculated using the Mark-Houwink equation with the constants for chitosan in the acetate buffer experimentally obtained by Yomota et al. [7]. In the range of molecular

weights $1.15 \times 10^3 < M < 1.59 \times 10^6$, the constants K and a equal to $0.199/\text{mL}\cdot\text{g}^{-1}$ and 0.59 , respectively, were used in calculations. For measuring the intrinsic viscosity, the classic Ubbelohde viscometer modified for foaming solutions with the capillary diameter of 0.42 mm was used [8].

2.4. Rheological Measurements

The rheological experiments were performed at room temperature, using a rheometer Physica MCR 501 (Anton Paar GmbH, Austria), equipped with an anti-slipping parallel-plate geometry. Viscoelastic properties in oscillatory shear flow were measured in the linear viscoelasticity region. The start-up tests at small shear frequencies were performed to investigate the dependence of solutions viscoelasticity on time. The measurements were started after 3 s pre-shearing at the shear rate 0.03s^{-1} , to ensure the same shear history for the measured samples. The homogeneous slurries with CS/CN proportion $70/30 \text{ wt. \%}$ containing 25 wt. \% of a plasticizer from the total content of CS and CN in the slurry were tested.

2.5. Scanning Electron Microscopy (SEM) and Transmission Electron Microscopy (TEM)

SEM was used to examine the surface structures of CS/CN films and their fractures. The observation was performed on field-emission gun scanning electron microscope Quanta 200 FEG (SEM; produced by FEI, Czech Republic) in the secondary electron mode at accelerating voltages of 5 kV . The samples were sputtered with platinum ($\sim 5 \text{ nm}$; Vacuum sputter coater SCD 050, Balzers) to avoid charging and sample damage due to electron beam.

TEM observations of CN dispersions were performed on a Tecnai G2 Spirit Twin 120kV (FEI, Czech Republic). The solution of bromophenol blue (0.1 wt. \%) was used as a color marker to increase the contrast of the chitin nanofibrils. A drop ($2 \mu\text{L}$) of the solutions was put onto a copper TEM grid (300 mesh) coated with a thin carbon film transparent for electrons. The excess of solution was sucked out by touching the bottom of the grid with filtering paper. This fast removal of the solution was performed after 1 min to minimize oversaturation during the drying process. The sample was left to dry completely at ambient temperature and then observed with a TEM microscope using bright field imaging.

2.6. Atomic Force Microscopy (AFM) of CS/CN Films in the Dried State

For characterizing the film surface at the micrometer and nanometer scale, atomic force microscopy (AFM) was applied for obtaining information about the surface topography and about the film properties, such as the surface heterogeneity. An Icon Dimension instrument, Bruker equipped with the SSS-NCL probe, Super Sharp Silicon™ - SPM-Sensor (NanoSensors™ Switzerland at the spring constant 35 Nm^{-1} with resonant frequency $\approx 170 \text{ kHz}$) was used. Measurements

were performed under ambient conditions using the tapping mode AFM technique. The scans covered the sizes from 0.35×0.35 to $30 \times 30 \mu\text{m}^2$. The upper and bottom surfaces of the samples were also analyzed.

2.7. AFM of CS/CN Films in the Swollen State

AFM characterization of CS/CN films was performed on Atomic Force Microscope Dimension ICON (Bruker). All images were acquired as topographical scans in Peak Force Tapping mode in water using silicon nitride tip ScanAsyst-Fluid (Bruker) with typical spring constant $k = 0.7 \text{ N/m}$ and scan rates within the range of 0.7–0.9 Hz. Prior to testing the CS supports CN adsorbed on their surface, they were double rinsed with fresh Milli-Q water to remove an excess of no adsorbed CN.

2.8. Sorption of Water Vapors

Water vapor sorption isotherms were determined by a gravimetric method using the sorption balance IGA-003 (Hidden Isochema, UK). In the used isothermal static procedure, the source of water vapors was liquid water added to the IGA reservoir. The film sample was loaded into the microbalance, weighed, and evacuated until constant weight was reached. After determining the mass of the dry sample, it was equilibrated at the isothermal temperature ($25 \text{ }^\circ\text{C}$). During the measurements, the pressure of water vapors was increased step by step to achieve the constant values equal to 5, 10, 15, 20, 25 or 30 mbar. At each pressure value, the saturated state of water vapors was reached. Values of each relative pressure at $25 \text{ }^\circ\text{C}$ were calculated using the software program, which also restricted the maximum pressure below condensation of water vapors. The amount of adsorbed water vapors (S_W) was evaluated as a percentage from the mass of a dry film.

2.9. Contact Angle Measurements

The hydrophobicity of CS/CN films was evaluated by the values of contact angles measured using an optical device OCA20 system (DataPhysics, Germany). The measurements were performed using the sessile drop method in the static mode. The samples have been prepared as follows: film disks (1.8 cm in diameter) were placed on a glass microscope slide and their borders were fixed in four points using double-sided Scotch tape (1 mm in diameter). Before measuring, all film samples were cleaned with compressed air. Both surfaces of the studied films were analyzed at least twice if difference between the measured values was high. Three to five $30 \mu\text{L}$ -drops of water were applied to each film disk at the rate of $5 \mu\text{L/s}$. Values of the contact angles were calculated based on the Young-Laplace fitting.

2.10. Thermogravimetric Analysis (TGA)

Thermogravimetric analysis (TGA) and differential scanning calorimetry (DSC) were used to characterize the thermal behavior of CN and CS/CN films. TGA measurements were performed on Perkin Elmer Thermogravimetric Analyzer Pyris 1 in air atmosphere to determine among others also the thermo-oxidative stability of the studied samples. The temperature interval of measurements was usually 30–800 °C, with gradual temperature rise of 10 °C/min and air flow 50 mL/min on samples of about 10 mg.

2.11. Measuring the Mechanical Characteristics of CS/CN Films

Tensile tests were carried out at ambient temperature using an Instron 5800 apparatus at a crosshead speed of 1 mm/min. At least eight specimens were tested for each sample. The stress-at-break, σ_b (variation coefficient < 2%), elongation at break, ε_b (variation coefficient < 5%), and Young's modulus, E (variation coefficient < 6%), were evaluated. Test specimens according to ISO with a length of working part 10 mm and width 2 mm were cut from cast films with thickness < 0.1 mm. The samples were conditioned in a hermetic box at 43% RH and 22 °C for 5 days before testing.

2.12. X-ray Diffraction Studies

Small Angle X-ray Scattering (SAXS) experiments were performed using a 3-pinhole camera (Molecular Metrology SAXS System now Rigaku). A X-ray beam produced by the microfocus X-ray tube (Bede Microsource) operating at 45 kV and 0.66 mA (30 W) was monochromized and focused by multilayer spherical optics (Osmic Confocal Max-Flux). SAXS patterns were measured using a multi-wire, gas-filled area detector with an active area diameter of 20 cm (Gabriel design). The probed q region was from 0.049 to 10.3 nm⁻¹, $q = (4\pi/\lambda) \sin(\vartheta)$, where $\lambda = 0.154$ nm is the wavelength and 2ϑ is the scattering angle. Data were always merged from two overlapping measurements in high- and low-resolution regions. Calibration was performed using Silver Behenate powder. Measurements took up to 2 h, depending on the quality and intensity of diffraction from sample.

3. Results and Discussion

3.1. Chitin Nanofibrils

The aqueous dispersions of CN (Figure 1a,b) resemble milky fluids. Their color may be different from slightly yellowish to brownish due to some admixture of carateno-protein components remaining bound to CN surface.

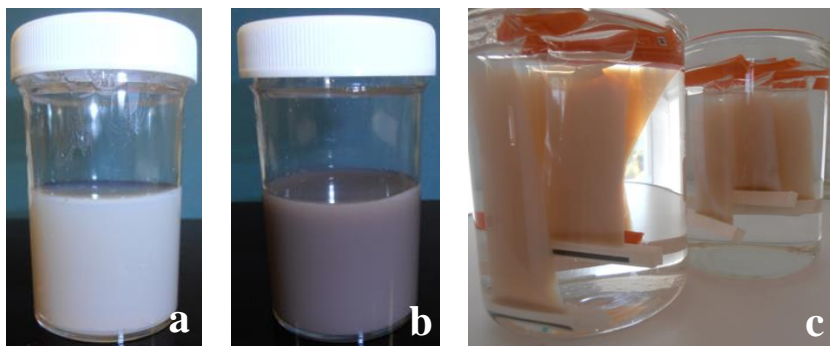


Figure 1. (a,b) Aqueous commercial dispersions of chitin nanofibrils (MAVI Sud Srl, Italy), (c) Clarification of commercial CN dispersions by dialysis against distilled water through 3.5-kDa SpectraPor dialysis cellulosic film. The precipitate and supernatant of CN were separated by centrifugation at 5000 rpm for 30 min.

The commercial CN dispersions (MAVI Sud Srl, Italy) contain sodium benzoate (0.5 wt. %) protecting them against microbial growth. As usual, the chitin nanofibrils do not precipitate at storage for at least a half a year but at their clarification by dialysis against distilled water (Figure 1c), a part of CN has been precipitated due to changing in the charge state of the CN surface after removal of the surface-adsorbed molecules of sodium benzoate. Initial pH of CN dispersions is shifted from acidic values (1.8–2) to more neutral (about 5.2–5.5), which are more favorable for aggregation of CN facilitating their precipitation.

The characterization of chitin nanofibrils in the swollen state was performed using AFM in the peak force tapping mode in water. In both precipitate (Figure 2a,c) and supernatant (Figure 2b,d), the CN had a spindle-like shape. They were slightly longer and thinner in the precipitate (Figure 2a,c) than in the supernatant (Figure 2b,d). The shape of CN in the swollen state was quite similar to that in the dried state (Figure 3a,b).

In AFM (Figure 2), SEM (Figure 3a) and TEM (Figure 3b) the average length of both swollen and dried CN did not exceed about 400–500 nm but their average diameter was about twice as small (about 35–40 nm) as that of the swollen CN (75–80 nm). The diameter of a single CN was considerably less (about 3 nm) [1]. It seems that the method of production of CN [4] has allowed the isolation of the chitin nanoparticles consisting of a higher quantity of bundles of nanofibrils.

We already know that the dimensions of CN have been affected by temperature and some salts such as CuSO_4 and $\text{Cu}(\text{CH}_3\text{COO})_2$. The effect of copper salts on the structure of CN has been enhanced with time and depends on the type of added salt. The copper sulfate molecules were able to fix on the CN surface (Figure 3b) without their destruction. When the CN supernatant was heated at 60 °C for 30 min

in the presence of copper acetate, the formation of bundles of single chitin chains was observed (Figure 3c).

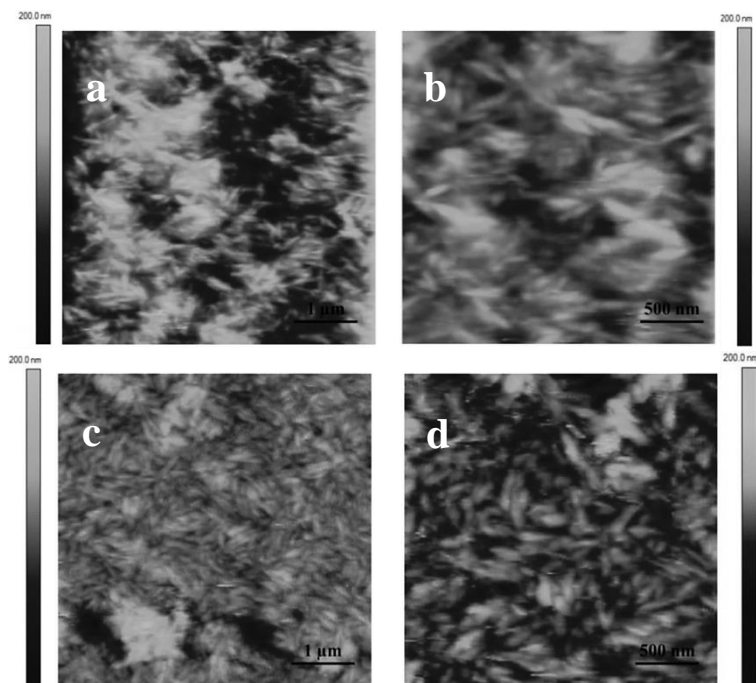


Figure 2. AFM images of CN in the swollen state in precipitate (a,b) and in supernatant (c,d). The scan size: $5 \times 5 \mu\text{m}$ (a,c) and $2.5 \times 2.5 \mu\text{m}$ (b,d). The CN were previously adsorbed on the surface of CS films during a day.

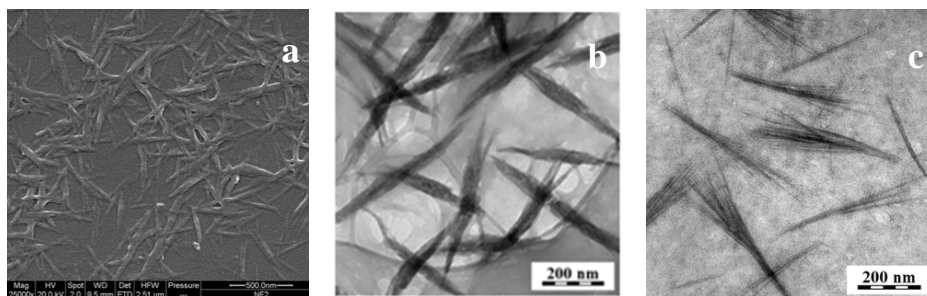


Figure 3. (a) SEM and (b,c) TEM images of dried CN: (a) initial (reprinted from [9]); (b) with surface-adsorbed CuSO_4 , and (c) heated at 60°C for 30 min in the presence of $\text{Cu}(\text{CH}_3\text{COO})_2$.

This is the clear evidence that some protein molecules enveloping the chitin chains are tightly fixed on the surface of CN. In the absence of metal salts, there were no essential changes of CN dimensions even during heating of CN supernatant free of metal salts at 60 °C for 1.5 h. Although the CN became thinner and somewhat shorter (Figure 4c,d vs. Figure 4a,b), their structure was not destroyed, and the reinforcing ability did not change.

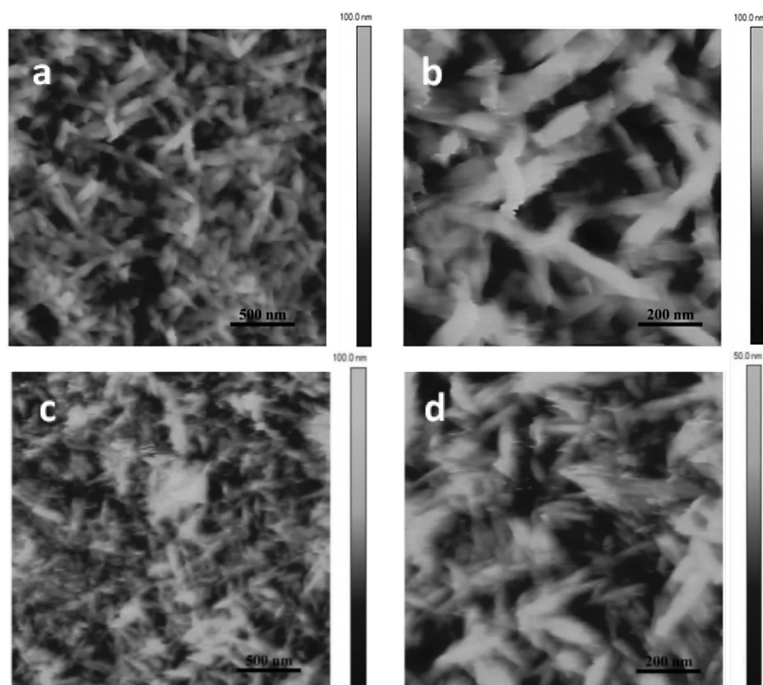
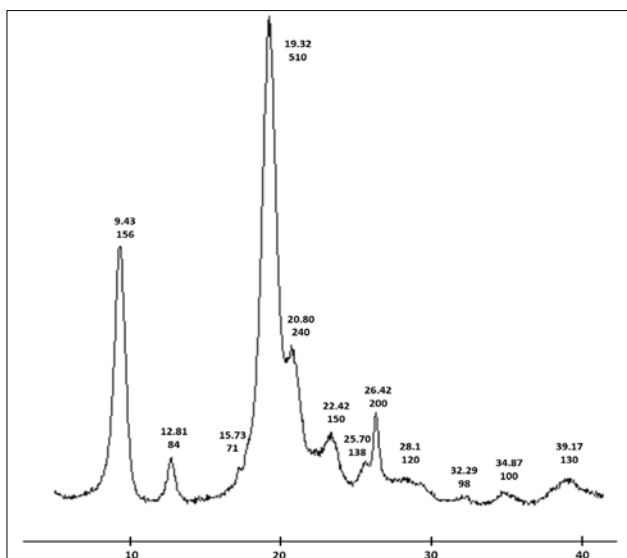


Figure 4. AFM topography images of CN in water: (a,b) initial supernatant, (c,d) after its heating at 60 °C for 1.5 h. The scan size: (a,c)— $2.5 \times 2.5 \mu\text{m}$, (b,d)— $1.0 \times 1.0 \mu\text{m}$. The CN were previously adsorbed on the surface of CS films during a day.

The crystallinity of CN [4] for all the samples has been tested by SAXS. The character of the X-ray diffraction pattern (Figure 5) is typical for a well-ordered crystalline phase.



Diffraction angle (in 2θ degrees)

Figure 5. The X-ray diffraction pattern of α -chitin nanofibrils. The upper and bottom digital labels (e.g., 9.43 and 156) at diffraction peaks denote the respective diffraction angle (in 2θ degrees for $\text{CuK}\alpha_{12}$) and X-ray intensity (in arbitrary scale), respectively.

Broadening of peaks corresponds to crystal imperfections due to different lengths of polysaccharide chains forming CN and due to small crystalline domains of nanofibrils. Positions of peaks uniquely identify the crystalline phase of α -chitin. This agrees (Table 1) with other observations [10].

Table 1. Characteristic peaks of the α -chitin nanofibrils in the X-ray diffraction pattern.

| Diffraction Angles (in 2θ Degrees) at the Main Peaks in X-ray Spectrum of α -Chitin | | | | | | | Reference |
|---|------|------|------|------|------|------|-----------|
| 1 | 2 | 3 | 4 | 5 | 6 | 7 | |
| 9.4 | 12.8 | 19.3 | 20.8 | 22.4 | 26.4 | 32.3 | Figure 5 |
| 9.2 | 12.6 | 19.2 | 20.6 | 23.2 | 26.2 | 32.2 | [10] |

The measured diffraction pattern of dried α -chitin (Figure 5) corresponds to the well-ordered crystalline polymer. It remains unchanged, i.e., the crystalline quality and average size of nanofibrils are identical no matter if the diffraction angle (in 2θ degrees) has been recorded on aqueous CN dispersion or dried CN flakes, on

a CN monolith or CS/CN plasticized or non-plasticized films. However, heating the aqueous CN dispersion in the presence of nitrates of such metals as Cu^{+2} , Be^{+3} and Ag^+ almost completely destroyed the crystallinity of CN.

3.2. Chitosan

As a rule, four production steps (demineralization, deproteinization, discoloration and deacetylation) are common for all manufacturers of chitosan from carapaces of crustaceans [9,11]. Nevertheless, the quality of various commercial chitosans can differ essentially because of the difference in the type of crustacean carapaces and in processing conditions (temperature, reaction time, concentration of alkali, pretreatment of the chitin and its concentration, particle size, concentration of dissolved oxygen and intensity of stirring). The variation of these parameters during the processing of chitin affects the properties of CS such as molecular weight and polydispersity of molecular distribution, the DA and solubility, content of mineral salts, and admixtures.

Usually, the targeted use of any packaging film determines the choice of raw materials, the quality of which must be sufficient for realization of this goal. One of the possible applications of completely biodegradable CS/CN films is, initially, one-off packaging for sandwiches, sliced cheese, or sausages, and, perhaps, packaging of food products with a short shelf life. Undoubtedly, the cost of such packaging film should be minimized because its price is included in the cost of packed products.

In our study, the cheap commercial CS of technical grade (Giusto Faravelli SpA, Italy) with molecular weight (M_W) 1425 ± 35 kDa determined by SEC and DA 21% was mainly used for preparation of CS/CN films. In some rheological experiments, the high-quality CS with M_W 425 kDa and DA 11% (HMC⁺ GmbH, Germany) was also tested.

Preliminary investigations have shown that the yellowish CS powder of the technical grade with sizes of particles from 0.1 mm up to 6 mm was not completely soluble at ambient temperature in distilled water acidified with acetic acid to pH = 4. After filtering the CS solution, the undissolved particles were retained on the surface of a non-woven polyester Histar filter (Figure 6a).

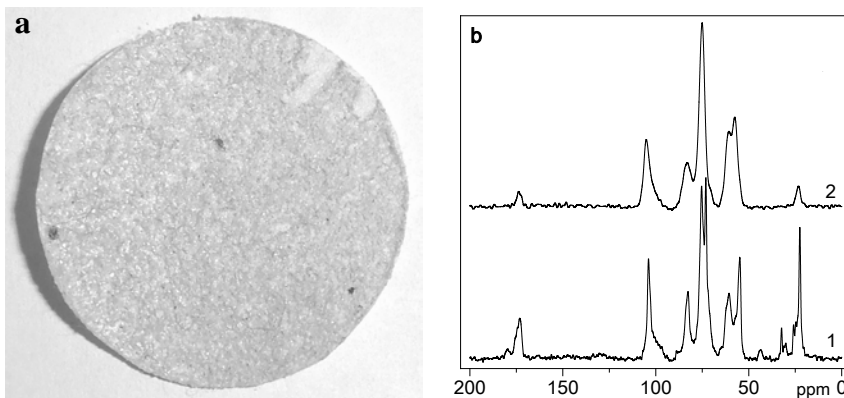


Figure 6. (a) Insoluble (at pH 4.0) CS particles retained on the non-woven Histar filter; (b) ^{13}C CP/MAS NMR spectra of insoluble and soluble CS (curves 1 and 2, respectively) at pH 4.3.

As was determined by the solid state ^{13}C CP/MAS NMR (Figure 6b), the insoluble particles with the DA value equal to 63% could be identified as chitin, since it is generally accepted that if the DA of the product is above 50 percent, it is characterized as chitin [12].

When prepared from raw chitosan solution, the composite CS/CN films contained additional microparticles (CM). In the SEM images (Figure 7a–c), these films looked unattractive from a commercial point of view because of both high roughness of their surfaces and morphological heterogeneity. Moreover, the films containing chitin microparticles together with CN were less mechanically stable (Table 2).

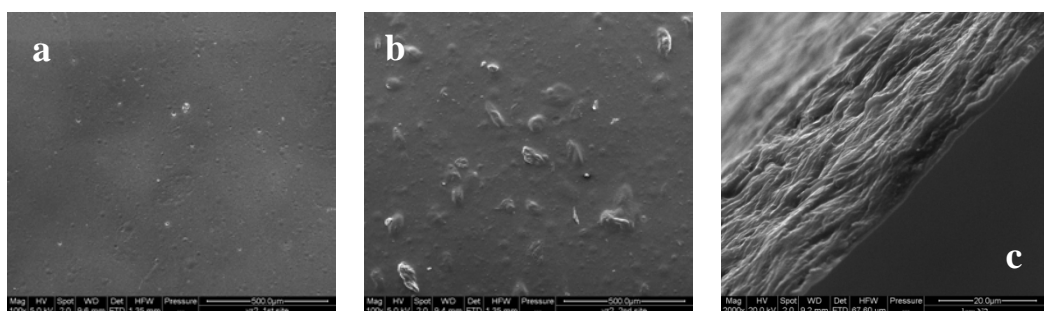


Figure 7. SEM images of (CS/CM)/glycerol film with the formulation: (40/60)/30 wt. %. (a,b) upper and bottom surfaces, respectively, (c) fracture of a film.

Table 2. Mechanical characteristics of the chitosan films containing CN or CM. Y—the Young's modulus; σ —the maximum tensile stress; ϵ —the strain at break of the film.

| Film | Formulation | Y, MPa | σ , MPa | ϵ , % |
|------------------|------------------|----------------|----------------|----------------|
| (CS/CN)/glycerol | (40/60)/30 wt. % | 3093 \pm 780 | 61.6 \pm 4.4 | 9.3 \pm 2.0 |
| (CS/CM)/glycerol | | 211 \pm 35 | 21.6 \pm 1.8 | 19.5 \pm 2.5 |

Therefore, to standardize the preparation process of the CS/CN films, the commercial CS powder was sieved through a set of standard sieves and two fractions with particles' dimensions less than 80 μm and (80–140 μm) were used.

Both CS and composite CS/CN films prepared from the sieved CS powder looked rather homogeneous. Nevertheless, they still contained some microparticles undissolved at pH 4.3 at the ambient temperature. To dissolve them completely, the CS solution had to be heated at least for an hour at 60 °C.

3.3. Rheological Behavior of CS/CN Slurries

The CS/CN slurry consisting of two phases—liquid (aqueous chitosan solution) and solid (chitin nanofibrils)—behaved as a structural viscoelastic liquid, the rheological properties of which depend on multiple interactions between the components [13].

In both aqueous CS solution and CN dispersion, there are both repulsive and attractive forces. In CS solution at pH 4–4.5, repulsion of protonated GlcN rings in some parts of CS chains dominates over attraction of GlcNAc rings in other parts of chains that prohibit the fast aggregation of CS molecules. The CN dispersions tend not to settle also for very long time, due to steric hindrance and repulsion of protonated GlcN rings existing on the surface of nanofibrils. Both systems, if they stand undisturbed during some time, are stabilized through the networks of multiple hydrogen bonds and hydrophobic interactions combining all constituents in each system. In CS/CN slurry, new interactions between CS chains and CN become dominant because of the high surface potential at the liquid/solid interface [14]. All these reasons are valid for freshly prepared CS solutions and slurries if their testing was carried out for two days but no longer, since the longer-term storage has caused irreversible changes of their rheological properties.

The rheological behavior of pure CS solution, CS/CN slurries without and with added plasticizers (glycerol, polyglycerol-3 or PEG-600) or saturated solutions of calcium, magnesium or barium hydroxides was investigated in detail [15]. These investigations were the basis for optimization of the composition and concentration of CS/CN slurries that, in turn, has led to improvement of the mechanical properties of composite films.

It was found that in all tested systems, the self-assembly process has ended by formation of *reversible thixotropic gels*, the characteristic feature of which was the loss of its internal microstructure in shear and the subsequent recovery in rest. Moreover, the CN appeared to be a strong gelling agent accelerating the self-assembly of slurries. In contrast, the addition of plasticizers retarded the formation of gel. Thus, e.g., for pure CS solution, the gel point has not been achieved even after 3.5 h-rest, whereas 28 min and 80 min were needed for gel formation of non-plasticized and PEG-600-plasticized CS/CN slurries, respectively [15]. The gel point of the slurries containing ions of the alkali-earth metals depended on the type of introduced metal ion. Ions of Ca^{+2} had the highest effect on the rate of gelation: in two glycerol-plasticized CS/CN slurries with and without Ca^{+2} ions, the gel has been formed after 12 min and 22min in rest, respectively. Ions of Mg^{+2} had delayed the formation of the plasticized gel up to 49 min. The effect of added Ba^{+2} on gelling the glycerol-plasticized CS/CN slurry was considerably stronger. The same pre-shearing conditions were insufficient for breaking the internal microstructure of the gel when saturated solution of barium hydroxide instead of calcium or magnesium hydroxides were added into CS/CN slurries (Figure 8).

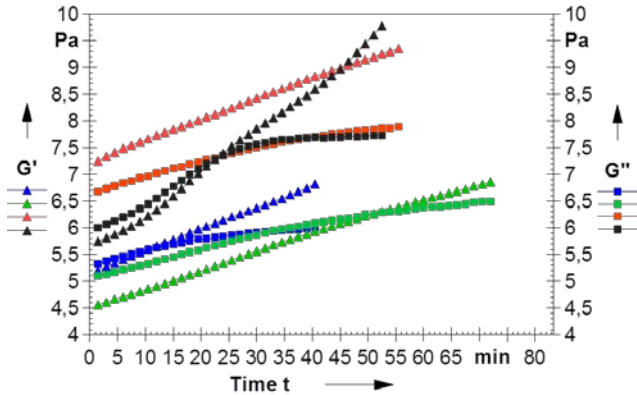


Figure 8. A self-organization process in the chitosan slurries—the storage G' and loss G'' dynamic moduli are plotted as functions of time: the slurry CS/CN/glycerol without metal ions (▲, ■), with Ca^{+2} ions (▲, ■), with Mg^{+2} ions (▲, ■), with Ba^{+2} ions (▲, ■).

In contrast to the loss modulus G'' being a measure of the energy dissipated in the slurry under the applied shearing deformation, the storage modulus G' characterizes the elastic deformation, at which the energy stored in a slurry under shear is then expended to return its parameters to the initial state when the shearing force is removed. For slurries containing transition metal ions, the values of the

storage modulus G' increase in the range: $\text{CS-Mg}^{+2} < \text{CS-Ca}^{+2} < \text{CS} < \text{CS-Ba}^{+2}$ that can be interpreted as an increase in springiness of the slurries.

The found thixotropic behavior of the slurry is a key factor at casting the CS/CN slurry on a template [15]. It characterizes the ability of the slurry to be easily applied to a surface during casting owing to breaking down of the microstructure of gel and rebuilding its viscosity in rest so that the coating does not drip and does not spread over the surface [13].

Among the most important rheological aspects describing the quality of coating is considered the *leveling*, which refers to the ability of slurry to flow laterally and diminish differences in thickness of adjacent areas of the coating, thus improving the smoothness, uniformity, and mechanical properties of CS/CN films.

The time lag for leveling of the cast slurry, after which its viscosity is restored, depends on viscosity of the slurry: the higher the viscosity, the slower leveling of coating. The time lag leveling was about 20 min for the slurries with the CS/CN proportion (70/30) wt. % plasticized with glycerol (30 wt. %), which have been used in preparation of CS/CN films.

An equally important parameter describing the rheological behavior of the slurry is the *yield stress* indicating the maximum value of the shear stress, at which the disruption of internal structure of the thixotropic CS/CN slurry will happen.

It was shown that some efforts (pre-shearing) must be applied to CS/CN slurries for disruption of their internal microstructures to force them to flow. The value of critical stress (*yield stress*) was about twice as high for the non-plasticized CS/CN slurry (6.8 Pa) than for plasticized ones with glycerol (3.9 Pa) or PEG-600 (3.1 Pa) if commercial CS (HMC⁺ GmbH, Germany) with low-molecular-weight (Mw 374 kDa) and low DA (11%) was used (Figure 9).

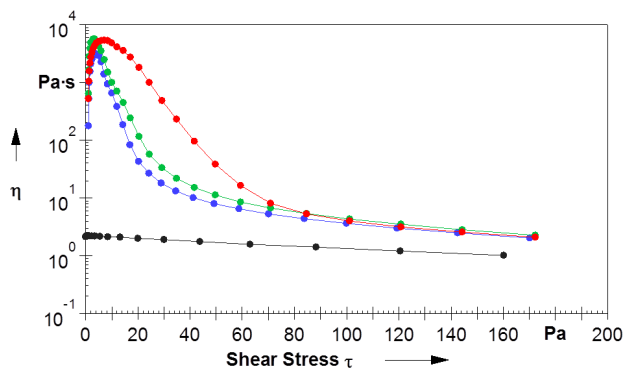


Figure 9. Steady shear viscosity vs. shear stress of the pure HMC⁺ chitosan solution (●) and the slurries: CS/CN (●), CS/CN/PEG (●), CS/CN/glycerol (●). The (CS/CN)/plasticizer proportion was (65/35)/30 wt. %.

Values of the yield stress of non-plasticized CS/CN slurry have increased about three times (up to 18.2 Pa) if the CS (Giusto Faravelli SpA, Italy) with higher molecular weight (1425 kDa) and DA (20%) was used. For CS/CN slurries plasticized with glycerol and polyglycerol-3, the yield stress was less and equal to 14.5 Pa independently on the plasticizer type (Figure 10).

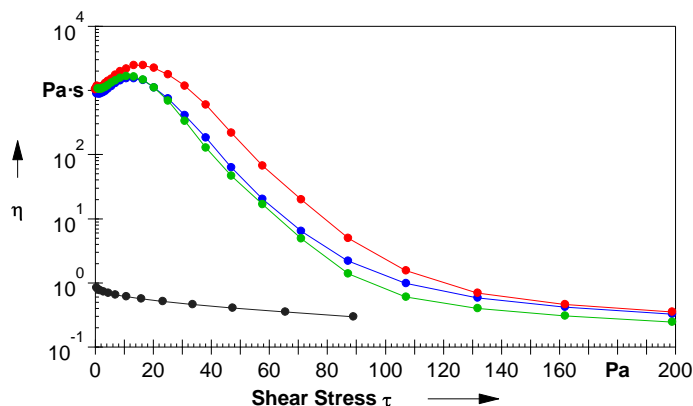


Figure 10. Steady shear viscosity as a function of the shear stress of the CS (Giusto Faravelli SpA, Italy) solution (●) and the slurries: CS/CN (●), CS/CN/glycerol (●), CS/CN/polyglycerol-3 (●). The (CS/CN)/plasticizer proportion was (70/30)/25 wt. %.

In both slurries, the CN dispersion (MAVI Sud Srl, Italy) with DA = 95% and pH = 5.12 has been mixed with CS solution. The slurries behaved as “fully” elastic fluids below the yield stress that had been manifested in their ability to absorb the shear energy as solids, which remain stationary, until the yield stress was not achieved. Above the yield stress, the internal microstructure has broken, and the slurries started to flow.

From a practical point of view, the gentle joggle or pulsed sonication of the CS/CN slurries could be effective for preventing the formation of their internal microstructure. It is reasonable to consider this recommendation for obtaining homogeneous coatings in the large-scale production of films using casting on the templates.

In this study, the homogeneous composite CS/CN films have been prepared from the slurry containing 70 and 30 wt. % of CS and CN, respectively, and 30 wt. % glycerol of total amount of CS and CN. The rheological parameters of this slurry (Figure 10, green curve) were determined as follows: the yield stress equal to about 15 Pa corresponded to the maximum steady shear viscosity about 1×10^3 Pa s.

Rheological testing provided useful information about rheological changes in time of the CS/CN slurries that allowed determination of the limit of their storage. The viscoelastic characteristics of the slurries had steadily getting worse. After their storage at 6 °C for 19 weeks, the slurries started to behave similarly to Newtonian fluids, the characteristic feature of which is the independence of their viscosity on the shear conditions (Figure 11).

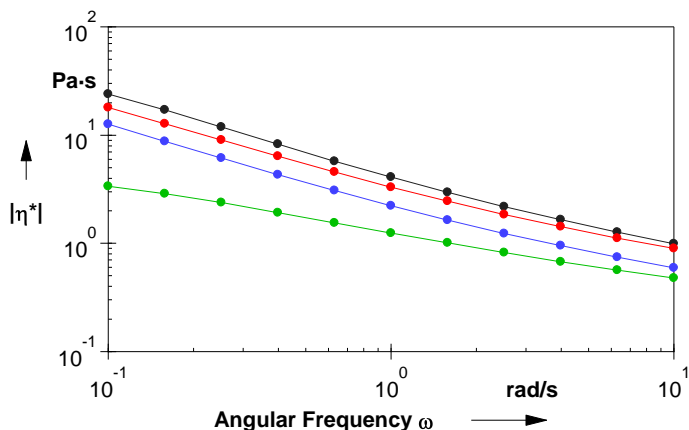


Figure 11. The absolute value of complex viscosity as a function of angular frequency of the slurry CS/CN/glycerol (70/30)/25 wt. % measured after various storage times: 1 day (●), 2 weeks (●), 6 weeks (●) and 19 weeks (●).

The absence of the rheological features typical for the physical network inside the slurries has indicated the clear evidence that CS chains had degraded into short fragments unable to form the extended microstructure of a thixotropic gel.

3.4. Composite CS/CN Films

The composite CS/CN films have been prepared by casting technique [16]. The used preparation procedure consisted of four steps (Figure 12).

Bearing in mind the effect of aging of CS/CN slurries on their rheology, its effect on the mechanical stability of the films has been also checked. It was found (Table 3) that all mechanical characteristics of the films worsened in strength the more significantly the longer the slurries were stored. Therefore, the slurries were always used as quickly as they were prepared.

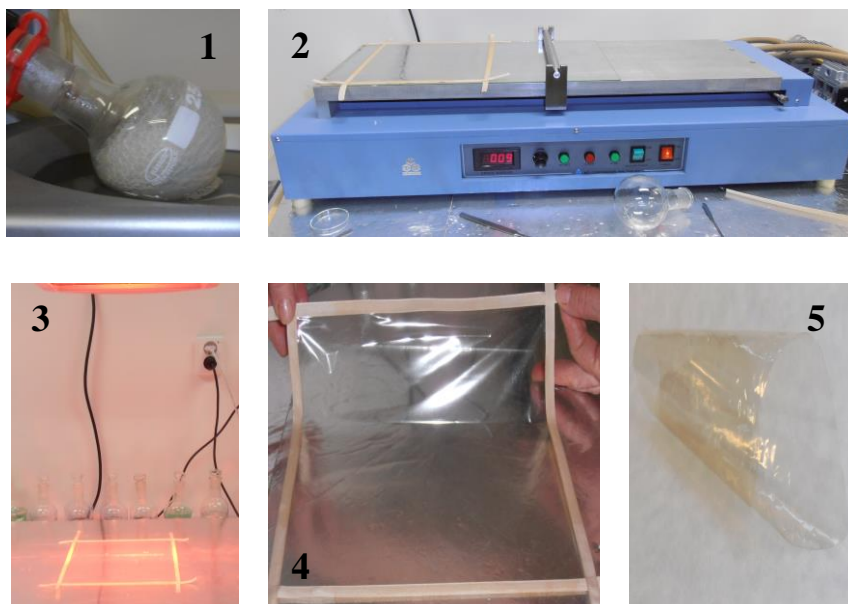


Figure 12. Visualization of the preparation steps of composite CS/CN films by casting technique. (1) deairing and concentrating the slurry using a rotary vacuum evaporator; (2) the slurry cast on a Dura Lar (Grafix Co., USA) support placed on a coater MSK AFA L800 (MTI Corp., USA) using a Doctor Blade; (3) drying the cast slurry by its heating at 50–55 °C using a source of the infrared light; (4) taking off the dried film from a support; (5) a died composite CS/CN film.

Table 3. Effect of the storage of a slurry on mechanical properties of (CS/CN)/glycerol films with the formulation: (70/30)/30 wt. %. I—used as prepared, pH = 4.25; II, pH = 4.43 and III, pH = 4.35—storage in fridge for 2 weeks and 1 month, respectively; The slurry II and III contained Ca^{+2} ions. The slurries II and III were additionally concentrated by vacuum evaporation prior to their casting on the supports.

| Parameter | I | II | III |
|-------------------|------------|------------|------------|
| Y, MPa | 2784 ± 582 | 460 ± 224 | 201 ± 44 |
| σ , MPa | 57.6 ± 5.9 | 37.8 ± 5.7 | 31.2 ± 4.9 |
| ε , % | 10.6 ± 2.4 | 25.2 ± 4.6 | 28.2 ± 3.2 |

It should be noted that vacuum evaporation used for mixing the aqueous solutions of the components, their deairing and concentrating allowed the preparation of very homogeneous slurries with desirable viscosity, which was close to the gel point but did not achieve it. This procedure took about a half of hour.

Evaporation of an excess of water from the slurry (about 25% from its weight) was carried out in a water bath with temperature at 60 °C.

The right choice of a support, on which the slurry is cast, becomes very important, if not the main factor in preparing the films of large dimensions. To avoid any defect in the dried film during its removal from the support, it is extremely important to use such a support, which will ensure easy removal of the dried film from its surface.

Some researchers were successful in preparation of experimental CS-based films having small dimensions when poly(vinyl chloride) sheets [17], polystyrene [18] or polypropylene plates [19], metallic [20] or non-stick trays [21], acrylic [22] or even Teflon [23] plates were used. Sometimes, the CS solutions were cast onto plastic [24] or glass [25] Petri dishes.

In our study, the CS/CN slurries have exhibited good adhesion to poly(vinyl terephthalate) films (Dura Lar, Grafix. Co., USA) and to stainless steel plates (Figure 13) and, at the same time, have ensured rather easy removal of the dried films from their surface by applying minimal efforts.

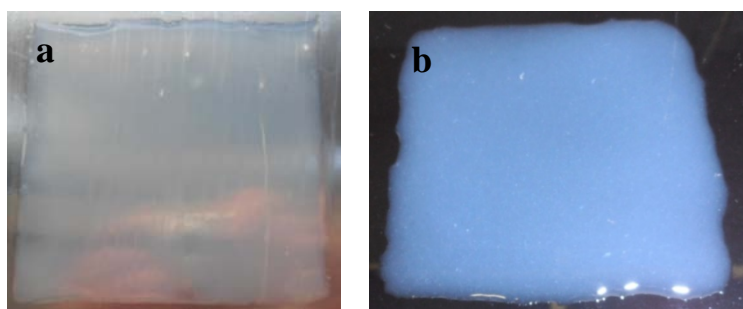


Figure 13. An optical view of the (CS/CN)/glycerol slurry at the proportion of components: (70/30)/30 wt. % cast on: (a) Stainless steel plate, (b) Dura Lar film.

The cast slurries on these supports formed uniform layers with thickness of about 0.75 mm. The thickness of dried CS/CN films plasticized with glycerol was equal to $46 \pm 16 \mu\text{m}$. For determination of the optimal formulation of the CS/CN slurry, the content of CN was increased from 3 wt. % to 40 wt. % (from the CS content). Chitin nanofibers introduced in CS solution promoted creating new spatial arrangement of chitosan chains in the dry CS/CN films, which differed considerably from the original one existing in the chitosan itself after its drying (Figure 14a–d). In aqueous acidified solution, the protonated CS chains preferred to interact with functional groups on the surface of rigid chitin nanofibrils than with each other. During the fixing on the surface of chitin nanofibers, the CS chains are packed more densely than in solution, acquiring a more energetically favorable spatial

arrangement. The reinforcing effect of CN on CS phase was ensured by a high surface potential of chitin nanofibrils with a highly developed surface (180 m^2 per 1 g of dried CN) [4]. The compatibility of CS with CN was excellent owing to similarity of their chemical structures differing only in the quantitative proportion of GlcN and GlcNAc rings and their distribution in polysaccharide chains. From the structural point of view, the CS/CN films can be considered to be composites consisting of one polymer. That is why there was no phase separation after increasing the content of CN in CS solution up to 80 wt. %. This newly formed interconnected spatial structure differed from the previous one in CS by the apparent new heterogeneity at the nano and micro level.

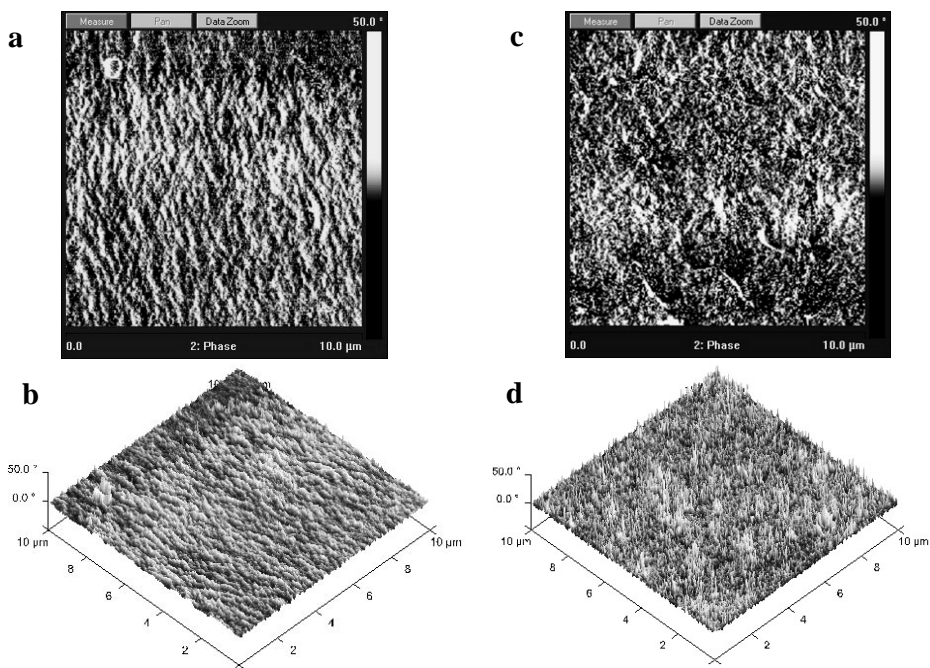


Figure 14. AFM phase images of the dry non-plasticized films: (a,b) CS; (c,d) (CS/CN) film at the proportion of components equal to (60/40) wt. %.

The increase in CN content in CS phase increased the stiffness of CS/CN films since the elastic deformation of the films has required applying stronger tensile stress at increase in CN content to a definite value (Figure 15). The ultimate tensile stress increased with CN content and achieved its maximum value for the CS/CN film with 10 wt. % of CN in CS solution. After further increase in CN content up to 40 wt. %, values of the maximum tensile stress decreased gradually. The effect of CN content on elongation of CS/CN films was the most perceptible. The value of

the strain at break of a film with 40 wt. % of CN was about half of that value of a chitosan film free of CN.

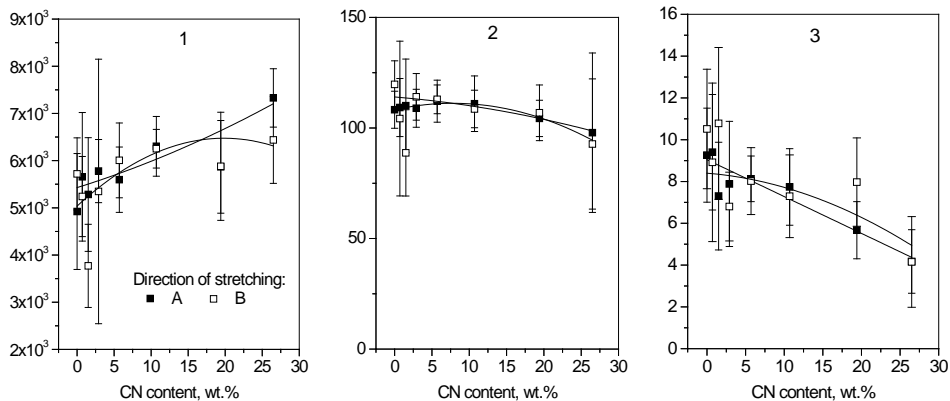


Figure 15. Effect of CN content in CS phase on the mechanical properties of non-plasticized films measured in two mutually perpendicular directions A and B of the applied tension. (1) Young's modulus; MPa, (2) Maximum stress, MPa; (3) Strain at break, %.

When the CN content exceeded 10 wt. %, the saturation limit of CS phase with CN was reached. An excess of CN was pushed out from CS phase and formed a surface-adjacent layer enriched with chitin nanofibrils (Figure 16).

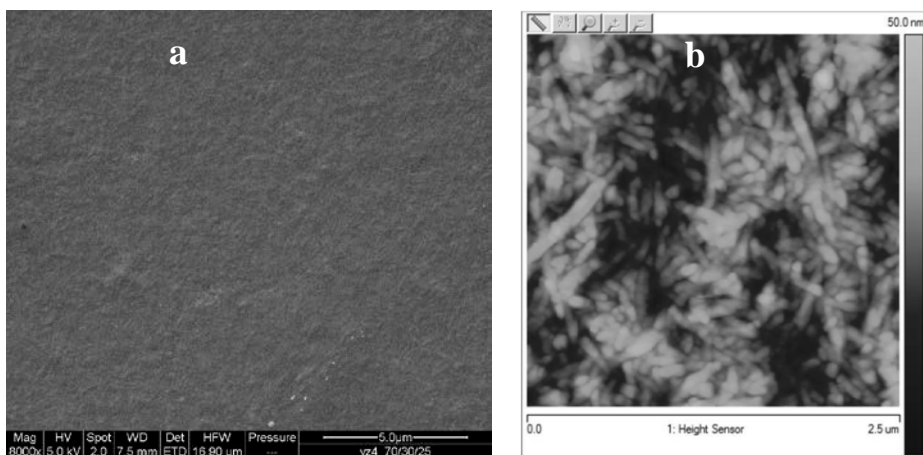


Figure 16. Images of the upper surface of a (CS/CN)/glycerol film at the proportion of components (70/30)/25 wt. % in the dry and swollen state in water. (a) SEM; (b) AFM images.

The bonds between chitosan chains and the surface groupings of chitin nanofibrils were so stable that the CS/CN films did not dissolve in water despite some excess of free molecules of acetic acid, which have remained inside the films after their drying. After dipping in water, the dimensions of CS/CN films reinforced with 30 wt. % of CN have increased only a little despite the presence of plasticizing glycerol molecules weakening interactions between the components in the films (Figure 17). However, an increase in the stiffness of the CS/CN films, especially those with high CN content, resulted in a decrease in their elasticity. Such film was more brittle.

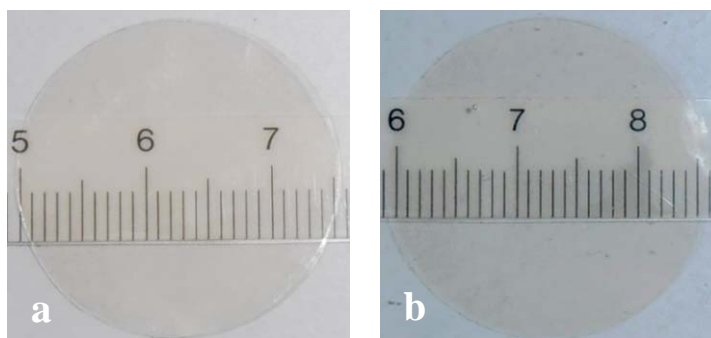


Figure 17. Dimensions of a (CS/CN)/glycerol film at the proportion of components (70/30)/25 wt. %. (a) dry film; (b) swollen film.

This problem is usually overcome by using plasticizers [26]. Small molecules of plasticizers penetrated between chitosan chains and weakened the bonds between them (Table 4). The comparison of the effect of the tested plasticizers on mechanical characteristics has shown that the elasticity of the CS/CN films increased considerably at the presence of a plasticizer and depended on both its quantity and its type.

For a film with the CS/CN proportion (85/15) wt. %, values of the elastic modulus decreased with increase in the plasticizer content in a great extent. Simultaneously, values of the ultimate tensile stress decreased for this film by about half but the values of its strain at break increased by about three-fold. It seems that it is not reasonable to increase the content of plasticizers higher than 20–30 wt. % because of dramatic worsening of all mechanical characteristics of CS/CN films.

The temperature of drying the CS/CN films was the next important parameter affecting their morphology (Figure 18) and mechanical characteristics (Table 5). The internal heterogeneity of CS/CN films became more pronounced when a cast slurry was dried using the infrared irradiation (Figure 18c,d) for half an hour instead of its drying at the ambient temperature (Figure 18a,b) for 12 h. The differences in

morphology of the dried films were observed on the micro level only. No noticeable differences in the appearance of the films were observed.

Table 4. Effect of type and content of a plasticizer on mechanical characteristics of CS/CN films with the formulation (85/15 wt. %). Support: Dura Lar film.

| Plasticizer, wt. % | | γ , MPa | σ , MPa | ϵ , % |
|--------------------|----|----------------|----------------|----------------|
| no | 0 | 5720 \pm 350 | 107.5 \pm 7 | 6.7 \pm 2.4 |
| Glycerol | 20 | 1390 \pm 600 | 43.0 \pm 5 | 20.4 \pm 4 |
| -- | 30 | 300 \pm 50 | 35.4 \pm 4 | 27.6 \pm 4 |
| -- | 40 | 50 \pm 12 | 17.0 \pm 6 | 36.0 \pm 4.5 |
| pG-2 | 20 | 1835 \pm 177 | 48.6 \pm 8 | 25.4 \pm 4.7 |
| -- | 30 | 700 \pm 65 | 36.7 \pm 5 | 32.5 \pm 5.7 |
| -- | 40 | 98 \pm 33 | 25.6 \pm 5.8 | 44.3 \pm 7.4 |
| pG-3 | 20 | 1390 \pm 100 | 33.5 \pm 6 | 26.7 \pm 8 |
| -- | 30 | 379 \pm 47 | 25.0 \pm 5 | 35.0 \pm 6 |
| -- | 40 | 65 \pm 8 | 24.4 \pm 4 | 50.0 \pm 4 |
| pG-4 | 20 | 2320 \pm 110 | 41.4 \pm 4.9 | 13.7 \pm 5 |
| -- | 30 | 1380 \pm 50 | 30.0 \pm 4.5 | 17.0 \pm 5 |
| -- | 40 | 370 \pm 57 | 28.6 \pm 6 | 31.6 \pm 7 |

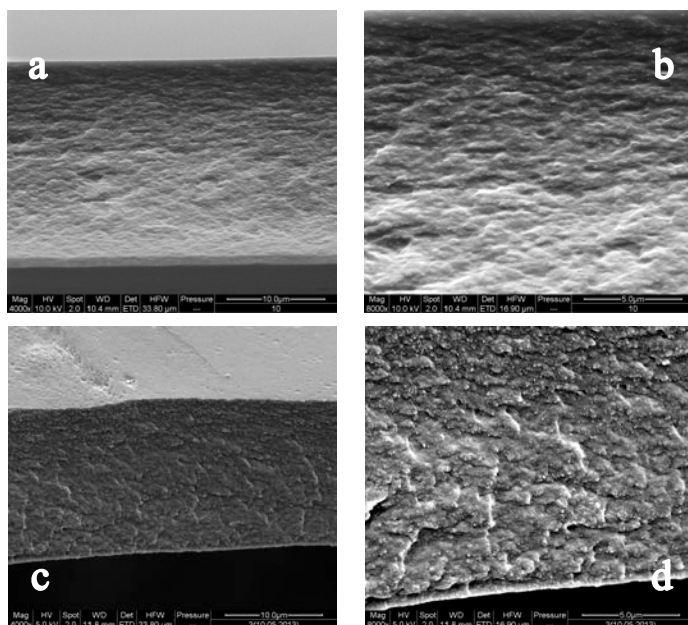


Figure 18. SEM images of fractures of (CS/CN)/glycerol films with the formulation (85/15)/30 wt. % dried at: (a,b) ambient temperature and (c,d) IR irradiation at 55 °C.

Table 5. Effect of the temperature of drying on the mechanical properties of (CS/CN)/glycerol films with the formulation (85/15)/30 wt. %.

| Parameter | 22–25 °C | 50–55 °C |
|-----------|------------|------------|
| Y, MPa | 1462 ± 306 | 2495 ± 380 |
| σ, MPa | 25.0 ± 3.6 | 45.0 ± 4.5 |
| ε, % | 12.6 ± 3.0 | 12.0 ± 3.0 |

Under exposition of the tested polysaccharides' films to UV light or microwave irradiation for 8 days and 30 min, respectively, the oxidative reactions were triggered inside the films. The fact of their existence was detected by analysis of UV spectra of the irradiated films (Figure 19).

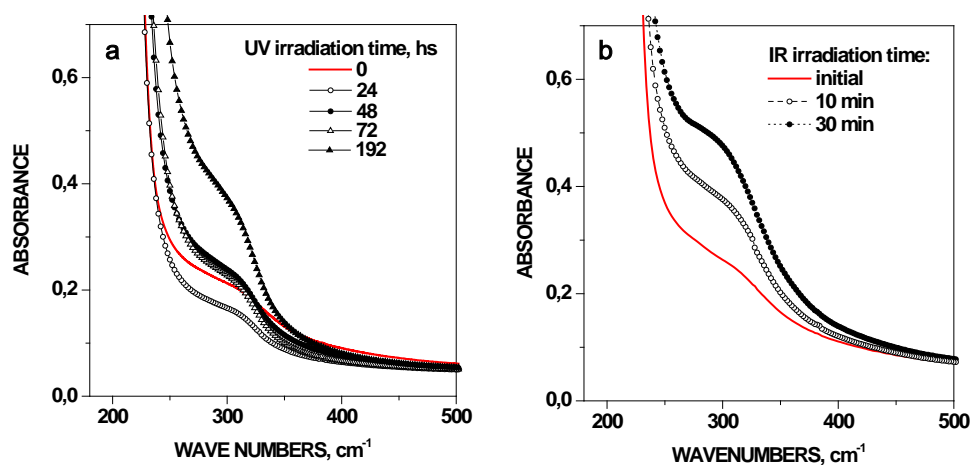


Figure 19. UV spectra of (CS/CN)/glycerol films after: (a) UV irradiation (0.5 N/m^2) for 192 hs and (b) microwave irradiation up to 30 min with the 1000 W-magneton power. The formulation of the slurries: (a) (40/60)/30 wt. %, (b) (20/80)/30 wt. %.

It is reasonable to suggest that drying the films using IR irradiation was also accompanied by accelerating the oxidative reactions in CS/CN films resulting in changes in packaging of CS chains that is manifested in morphological changes of the films (Figure 20c,d).

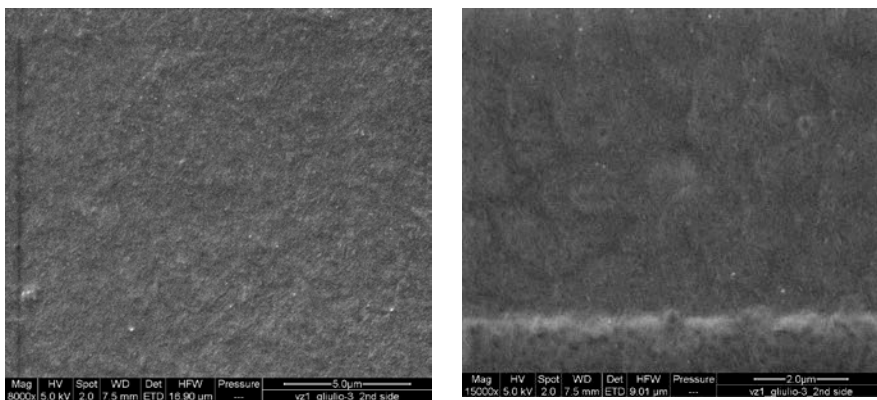


Figure 20. SEM images of the bottom surface of (CS/CN)/glycerol film with the formulation (70/30)/25 wt. % obtained by casting the slurry on a stainless steel plate.

Investigations of the degradation of CS/CN films at the elevated temperatures by thermogravimetric analysis (Table 6) has revealed that CN consisting of the densely packed chitin chains required higher temperatures than raw CS powder or reprecipitated CS. It should be noted that a sample of reprecipitated CS has lost 40% of its mass within a very narrow temperature interval with its maximum at 306 °C. This value was about 12 °C higher than the temperature maximum on a TGA curve of the raw CS. It means that to improve the thermostability of raw CS, the reprecipitation could be used to remove low-molecular-weight oligosaccharides and increase the fraction of high-molecular-weight CS. The decomposition of chitin nanofibrils occurred at temperature approximately 50 °C higher than that of CS.

It is interesting that two maximums on TGA curves of CS/CN films have been observed. The decomposition temperature of the films rose to higher values (for the first and second decomposition steps from about 304 to 311 °C and from 361 to 371 °C, respectively) with the increase in CN content from 15 wt. % to 35 wt. %. The loss of the mass of a sample decreased from 30% to 23% for the first degradation step. Simultaneously, at the second degradation step, the loss of the mass of a sample increased from about 20% to 26%. For CS/CN films having the same formulation (85/15)/30 wt. % but containing polyglycerols of different type, the higher temperature was required for decomposition of the film plasticized with polyglycerol-4 having longer molecules. For CS/CN films plasticized with polyglycerol-3, the decomposition temperature rose with an increase in the content of plasticizer at both steps of their degradation. The detailed description of TGA and DSC analysis of the composite films based on CS and CN will be published elsewhere.

Table 6. TGA analysis of CS, CN, and composite CS/CN films. T1, T2, T3 – temperature, °C. $\Delta W1$, $\Delta W2$, $\Delta W3$ – loss of a sample's weight, wt. %.

| Sample | Composition | T1 | $\Delta W1$ | T2 | $\Delta W2$ | T3 | $\Delta W3$ |
|--------------|-------------|-------|-------------|-------|-------------|-------|-------------|
| CS raw | | 294.4 | 47 | – | – | – | – |
| CS * | | 306.0 | 40 | – | – | – | – |
| CN | | 358.2 | 66 | – | – | – | – |
| CS/CN | 85/15 | 303.7 | 30 | 360.9 | 19.5 | – | – |
| –“–“–“– | 75/25 | 306.5 | 28 | 371.0 | 22.0 | – | – |
| –“–“–“– | 65/35 | 310.9 | 23 | 370.9 | 25.5 | – | – |
| (CS/CN)/pG-2 | (85/15)/30 | 261.5 | 22.5 | 315.4 | 23.5 | 384.5 | 18.0 |
| (CS/CN)/pG-3 | –“–“–“– | 303.4 | 40.0 | 374.6 | 19.5 | – | – |
| (CS/CN)/pG-4 | –“–“–“– | 304.4 | 41.0 | 385.2 | 21.0 | – | – |
| (CS/CN)/pG-3 | (85/15)/20 | 314.1 | 37 | 384.8 | 18.0 | – | – |
| –“–“–“– | (85/15)/30 | 312.0 | 41.0 | 384.6 | 17.5 | – | – |
| –“–“–“– | (85/15)/40 | 304.9 | 55.5 | 401.1 | 17.5 | – | – |
| –“–“–“– | (85/15)/50 | 305.7 | 63.0 | 400.0 | 12.0 | – | – |

Analyzing the SEM images in Figure 20, everyone can clearly see that the (CS/CN)/glycerol films have denser upper and bottom layers and moreover, the film surface facing a support seems to be considerably denser than that contacting with air.

It was observed (Table 7) that not only the type of the surface (upper or bottom) of CS/CN film but also the chemical nature of a support on which it was formed remarkably affected the values of contact angles of both film surfaces. As a rule, the values of contact angles of the bottom surfaces were higher than those of the upper ones exposed to air. In contrast to the transparent glycerol-plasticized CS/CN films formed on the Dura Lar supports from poly(vinyl terephthalate), those formed on the stainless steel plates looked matte because of higher surface roughness of the latter support (Figure 20).

Table 7. Contact angles of the surfaces of glycerol- or pG-3-plasticized CS/CN films.

| Surface | Support | DL | SS | DL | SS | DL | SS |
|---------|---------|-----------------|-------------|--------------|-------------|-------------|-------------|
| | | Non-plasticized | | 30% Glycerol | | 30% pG-3 | |
| Upper | | 102.2 ± 4.4 | 105.6 ± 2.7 | 105.2 ± 5.1 | 106.5 ± 3.5 | 103.2 ± 4.1 | 104.7 ± 1.8 |
| Bottom | | 107.1 ± 3.8 | 125.2 ± 4.8 | 107.0 ± 3.8 | 115.4 ± 2.6 | 106.5 ± 3.9 | 109.7 ± 0.6 |

The chemical nature of a support, on which the slurry was cast, influenced also the composition of chemical groupings on the formed film surface. The X-ray photoelectron spectroscopy analysis of both surfaces of glycerol-plasticized CS/CN films, which differed in formulations (Table 8), has revealed that the hydrophilic groupings (–C–O–, –C–O–C– and –N–C=O–) were predominantly located on the

upper surface of the films. In contrast, the bottom surfaces formed on the glass plates silanized with ethyltrimetoxysilane had more hydrophobic groupings ($-C-C-$ and $-C-H-$).

Table 8. Binding energy of chemical groupings in the spectra of C 1 s electrons.

| Binding Energy, eV | (CS/CN)/Glycerol Proportion, wt. % | | | | Chemical Groupings |
|--------------------|------------------------------------|--------|------------|--------|-----------------------|
| | (80/20)/20 | | (60/40)/40 | | |
| | Upper | Bottom | Upper | Bottom | |
| 285.0 | 29 | 37 | 28 | 33 | $-C-C-$; $-C-H-$ |
| 285.6 | 9 | 10 | 10 | 10 | $-C-NH_2$ |
| 286.6 | 52 | 46 | 50 | 47 | $-C-O-$ |
| 288.2 | 10 | 7 | 12 | 10 | $-C-O-C-$; $-N-C=O-$ |

The surface wettability of CS/CN films with water (Figure 21) depended on both chemical groupings on the surface of films and on the density of packaging of their structural elements.

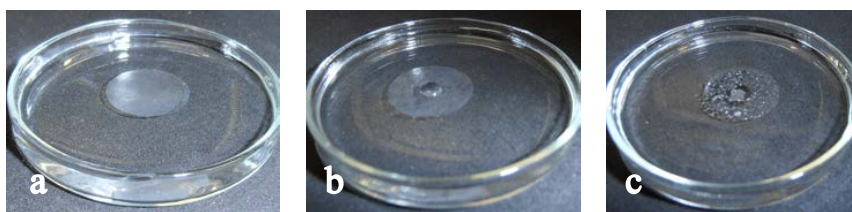


Figure 21. Wettability of a (CS/CN)/glycerol film with the formulation (75/25)/30 wt. %: (a) just after placing on the water surface; (b,c) after 5-min- or 2-h contact with water, respectively.

The suction of water inside such films occurred when the content of an admixture of low-molecular-weight chitooligosaccharides together with some excess of the acetic acid molecules were high and these components have transferred into water creating the channels inside the films dipped into water. This phenomenon was often observed when CS solution was heated at 60 °C for one hour to dissolve small CS microparticles for obtaining homogeneous slurry or when the slurry has been stored in the fridge for two days.

It should be noted that despite good wettability, these films did not dissolve in water and did not change their size during at least 10 days of contact with water.

Both high permeability and adsorption of water (Table 9) have been also detected for the CS/CN films containing the ions of alkali earth metals such as Ca^{+2} , Mg^{+2} or Ba^{+2} . Freshly prepared saturated solutions of hydroxides of these metals free of

carbon dioxide were added to CS/CN slurries with the aim of neutralizing an excess of the acetic acid used for dissolving of CS at preparation of the slurries.

Table 9. Adsorption of water vapors with CS/CN films.

| Film | Components | Support | Composition | | S _w , wt. % | | $\frac{S_{192}}{S_{w1}}$ |
|------|------------------------------------|---------|-------------|--|------------------------|----------------------|--------------------------|
| | | | wt. % | | Air-Dried ¹ | Swollen ² | |
| 1 | (CS/CN)/PEG-600 | DL | (70/30)/25 | | 7.6 | 25.2 | 3.3 |
| 2 | (CS/CN)/glycerol | — — — | (75/25)/30 | | 5.3 | 24.8 | 4.7 |
| 3 | (CS/CN)/pG-3 | — — — | (85/15)/30 | | 7.4 | 20.8 | 2.8 |
| 4 | — — — | — — — | (75/25)/30 | | 6.8 | 33.5 | 4.8 |
| 5 | — — — | — — — | (65/35)/30 | | 5.5 | 32.5 | 6.1 |
| 6 | (CS/CN)/glycerol, Ca ⁺² | DL | (70/30)/25 | | 45.2 | 38.1 | 0.8 |
| 7 | — — — | SS | — — — | | 43.9 | 35.7 | 0.8 |
| 8 | (CS/CN)/glycerol | DL | (70/30)/10 | | 8.3 | 22.3 | 2.7 |
| 9 | — — — | SS | — — — | | 6.8 | 24.0 | 3.5 |
| 10 | (CS/CN)/glycerol, PGPR | DL | (70/30)/30 | | 7.2 | 20.0 | 2.8 |
| 11 | — — — | SS | — — — | | 6.0 | 25.1 | 4.2 |
| 12 | (CS/CN)/glycerol, PLA | DL | (70/30)/30 | | 10.3 | 22.2 | 2.2 |
| 13 | — — — | SS | — — — | | 8.4 | 21.8 | 2.6 |
| KFC | cellulose | | | | 5.4 | 13.0 | 2.4 |

Comparison of the air-dried CS/CN films has shown that the water content was always higher in the films prepared using Dura Lar supports than in those obtained using the stainless-steel plates. The content of water in CS/CN films plasticized with polyglycerol-3 decreased with the increase in CN content from 15 to 35 wt. %. The CS/CN films with the surface-adsorbed polyglycerol polyricinoleate or polylactide had lower water content if the stainless-steel plates instead of Dura Lar ones have been used as the support for casting the slurry. The glycerol-plasticized CS/CN films containing calcium ions retained the highest amount of water in the air-dried state. Most of this water was bound with metal ions in their hydration shells. At equilibrium with water vapors at 25 mbar, the saturation state was not achieved for these films and they contained only 80% of water from its content in the air-dried films. In the sorption experiments, the sorption of water proceeded slowly by the films and took several hours until equilibrium with water vapors was achieved at each partial pressure. Being equilibrated with water vapors at 25 mbar, the swollen CS/CN films contained from 3 to 5 times more water than the air-dried ones. In the moistened state, the CS/CN films prepared by casting the slurry on the stainless-steel plates contained more water than those obtained by using Dura Lar supports. This difference can be explained by the structural differences of the films.

These are the structural features of the films that determine the dependence of the change in the moisture vapor transmission rate through a film on its equilibrium state at each change of the partial pressure of water vapors (Table 10).

Table 10. Moisture vapor transmission rate for the (CS/CN)/glycerol film with the formulation (70/30)/30 wt. %. The film contained 0.234 mmol of Ca⁺² ions.

| Δp , mbar | 0–0.45 | 0.45–5.2 | 5.2–10.4 | 10.4–15.4 | 15.4–20.3 | 20.3–25.3 |
|---------------------------------|--------|----------|----------|-----------|-----------|-----------|
| MVTR, g/(m ² × 24 h) | 4.1 | 31.6 | 65.1 | 111.5 | 186.1 | 180.1 |
| $\Delta MVTR/\Delta p$ | 9.1 | 6.1 | 6.3 | 7.2 | 9.2 | 7.1 |

At low water vapor pressures, the rate of MVTP change ($\Delta MVTR/\Delta p$ value) was high since water molecules have adsorbed onto the outer surfaces and on the surface of the available pores of a dry film free from any adsorbed water at zero pressure of water vapors in the apparatus chamber at the beginning of the sorption process.

When the partial water vapor pressures achieved 15.4 mbar the second increase in the rate of MVTR changing occurred due to the changes of packaging the CS chains and the increase in the distance between them in the moistened film.

The difference in distance between CS chains in the dry and swollen films influenced their permeability for gases (Table 11). The permeability of hydrogen, oxygen and nitrogen through a swollen glycerol-plasticized CS/CN film was about triple higher than that of the dry film. The molecules of carbon dioxide penetrated through the swollen film about five times faster compared with the dry film. Comparison of the kinetic diameters and molecular mass of gases with the rate of their transfer through a CS/CN film allows us to conclude that the decisive factors defining the film permeability (P) for gases are their diffusivity (D) and solubility (S) controlled by numerous interactions of the diffusing molecules inside the CS/CN films.

Table 11. Permeability of a (CS/CN)/glycerol film with the formulation: (70/30)/25 wt. % for gases.

| Film | P | H2 | O2 | N2 | CO2 | CH4 |
|------------------|--------|-------|-------|-------|-------|------|
| Dry | barrer | 0.04 | 0.012 | 0.005 | 0.142 | 0.01 |
| Swollen | | 0.137 | 0.038 | 0.013 | 0.761 | – |
| Kinetic diameter | Å | 2.89 | 3.46 | 3.64 | 3.30 | 3.8 |
| Molecular mass | D | 2 | 32 | 28 | 44 | 18 |

Analysis of the transfer of oxygen through the composite films with the same content of CS and CN but containing various plasticizers has elucidated the correlation between the structure of the composite films and their permeability for gases.

The most permeable for oxygen were the films plasticized with PEG-600 (Table 12). The permeability and the diffusion coefficient of oxygen in these films were about three and five orders, respectively, higher than those of the films plasticized

with glycerol. In contrast, the solubility of oxygen in the former films was about three orders lower than that in the latter ones. High diffusivity together with low solubility of oxygen in the PEG-plasticized films ensured their high permeability. The observed differences in the transport performance of the films were determined by the difference in their spatial structures, on which the different plasticizers were affected in different ways.

Table 12. Oxygen transport through dry plasticized CS/CN films with the formulation: (70/30)/30 wt.% * 1 barrer = $1 \times 10^{-10} \text{ cm}^3 \text{ (STP)} \times \text{cm} / (\text{cm}^2 \times \text{s} \times \text{cm Hg})$ [27,28].

| Film | P | | D | S |
|------------------|---|---------|------------------------|----------------------------------|
| | 10^{18} mol/(m \times Pa \times S) | barrer* | 10^{15} m 2 /s | 10^6 mol/(m $^3 \times$ Pa) |
| (CS/CN)/PEG-600 | 172 | 0.512 | 1.21×10^6 | 0.14 |
| (CS/CN)/glycerol | 0.18 | 0.00054 | 2.25 | 80.7 |
| (CS/CN)/pG-2 | 1.28 | 0.0038 | 14.4 | 88.7 |
| (CS/CN)/pG-3 | 1.21 | 0.0036 | 25.9 | 46.8 |
| (CS/CN)/pG-4 | 0.13 | 0.00037 | 2.43 | 51.7 |

For decreasing wettability and permeability of CS/CN films for water vapors, the hydrophobization of their surfaces was carried out.

This procedure was performed by dipping the films into dioxane solution of polylactide (PLA) with molecular mass of 7.7 kDa or polyglycerol polyricinoleate (PGPR) for half an hour. Both surfaces of the plasticized CS/CN film treated in such a way have acquired their water-repellent properties (Figure 22) and simultaneously their mechanical characteristics were considerably improved.

The effect of surface modifiers on the mechanical characteristics of (CS/CN) films containing various low- and high-molecular-weight substances are summarized in Tables 13–16. From the results (Table 13), we can get an idea of the effect of glycerol, gelatin, and CN on the magnitudes of the elastic modulus (Y), the ultimate stress (σ) and the strain at break (ϵ) of the CS-based films. In contrast to glycerol being the disintegrating agent for the CS phase, gelatin molecules have combined the CS chains promoting their tighter packaging but the introduction of glycerol in the CS/gelatin slurry-2 caused another disintegration of the formed intermolecular bonds.

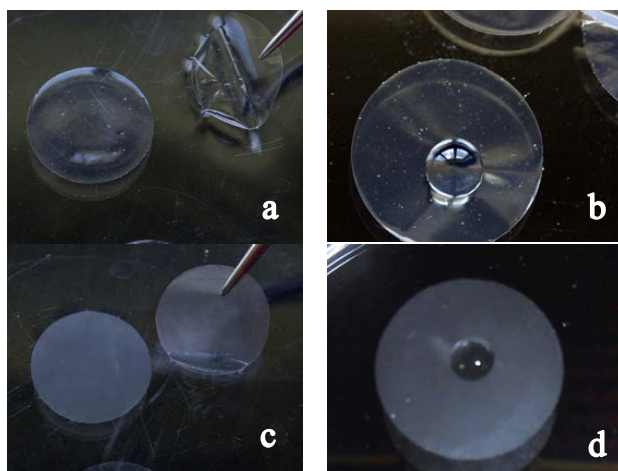


Figure 22. Photos of PLA-modified (CS/CN)/glycerol film with the formulation: (70/30)/30 wt. %. The slurry was cast on: (a,b) Dura Lar support; (c,d) stainless steel plate.

Table 13. Mechanical characteristics of CS-based films with different formulations.

| Slurry | Components | Formulation | Y, MPa | σ , MPa | ϵ , % |
|--------|-----------------------------|-----------------|------------|----------------|----------------|
| 1 | CS/glycerol | 70/30 | 1442 ± 55 | 34.0 ± 3.5 | 18.8 ± 2.9 |
| 2 | CS/gelatin | 90/10 | 3702 ± 129 | 69.9 ± 3.3 | 4.9 ± 2.2 |
| 3 | (CS/gelatin)/glycerol | (90/10)/30 | 1714 ± 79 | 35.5 ± 4.2 | 16.7 ± 4.4 |
| 4 | [(CS, gelatin)/CN]/glycerol | [(90/10)/25]/15 | 3000 ± 164 | 55.3 ± 5.0 | 14.3 ± 2.5 |
| 5 | —“—“—“—“— | [(90/10)/25]/25 | 1263 ± 544 | 36.9 ± 6.1 | 16.2 ± 4.4 |
| 6 | —“—“—“—“— | [(90/10)/30]/30 | 325 ± 48 | 33.3 ± 7.1 | 18.7 ± 3.9 |

Table 14. Mechanical characteristics of (CS/CN)/glycerol films with the formulation: (70/30)/30 wt. % with 0.234 mmol Ca(OH)₂ and 0.1 mmol Ca₃(PO₄)₂ or with 10 wt. % gelatin from CS amount.

| Parameter | Additive | | Gelatin | | | Ca(OH) ₂ , Ca ₃ (PO ₄) ₂ | | |
|----------------|------------|------------|------------|------------|-------------|---|--|--|
| | None | PLA | PGPR | None | PLA | PGPR | | |
| Y, MPa | 634 ± 95 | 3993 ± 447 | 4032 ± 264 | 176 ± 42 | 670 ± 246 | 1363 ± 868 | | |
| σ , MPa | 36.1 ± 4.3 | 61.1 ± 8.6 | 58.8 ± 1.9 | 20.3 ± 5.8 | 53.8 ± 11.2 | 42.9 ± 6.7 | | |
| ϵ , % | 20.3 ± 2.2 | 11.8 ± 2.9 | 12.2 ± 1.4 | 19.7 ± 5.8 | 20.6 ± 5.2 | 15.4 ± 2.7 | | |
| θ , ° | 93.2 ± 1.3 | 95.1 ± 3.1 | 99.3 ± 3.2 | 94.1 ± 0.1 | 96.8 ± 2.4 | 100.9 ± 2.4 | | |
| SW, % | 23.8 | ND | ND | ND | 37.2 | ND | | |

Chitin nanofibers, which are powerful reinforcing agents, have leveled the disintegrating effect of the plasticizer at its small amount in slurry 4 (Table 13). However, all mechanical characteristics of the composite films have dramatically worsened with increasing content of glycerol in slurries 5 and 6.

The mechanical characteristics of the composite films obtained from slurry 6 were practically restored after their modification with polylactide (PLA) or polyglycerol polyricinoleate (PGPR) (Table 14).

Table 15. Mechanical characteristics of (CS/CN)/glycerol films with the formulation: (70/30)/30 wt. % with 5 wt. % monolignols or 1 wt. % nanolignin from CS amount. Surface modifier: PLA—polylactide, 7.7 kDa or PGPR—polyglycerol polyricinoleate.

| Parameter | Monolignols | | | Nanolignin | | |
|--------------------|----------------|------------|-------------|------------|------------|------------|
| | None | PLA | PGPR | None | PLA | PGPR |
| Y, MPa | 293 ± 66 | 3503 ± 457 | 3236 ± 472 | 455 ± 56 | 3883 ± 405 | 4027 ± 400 |
| σ, MPa | 26.3 ± 3.6 | 57.1 ± 9.8 | 45.9 ± 9.8 | 24.1 ± 3.7 | 51.4 ± 4.9 | 50.9 ± 4.9 |
| ε, % | 20.8 ± 3.2 | 13.1 ± 2.7 | 14.7 ± 1.6 | 14.6 ± 2.4 | 10.9 ± 2.2 | 12.9 ± 2.0 |
| θ, ° | 96.0 ± 1.7 | 96.5 ± 1.2 | 104.9 ± 3.2 | | | |
| S _w , % | Not determined | | 21.5 | | | |

Table 16. Mechanical characteristics of (CS/CN)/glycerol film with the formulation: (70/30)/30 wt. % with 0.178 mmol Mg⁺², 0.234 mmol Ca⁺² or 0.321 mmol Ba⁺² ions.

| Parameter | PGPR | | | PLA | | |
|-----------|------------------|------------------|------------------|------------------|------------------|------------------|
| | Mg ⁺² | Ca ⁺² | Ba ⁺² | Mg ⁺² | Ca ⁺² | Ba ⁺² |
| Y, MPa | 3987 ± 134 | 2807 ± 186 | 2535 ± 506 | 3940 ± 200 | 3597 ± 271 | 3034 ± 262 |
| σ, MPa | 67.2 ± 7.2 | 55.1 ± 5.6 | 49.6 ± 9.8 | 65.1 ± 4.7 | 62.9 ± 5.2 | 55.9 ± 5.6 |
| ε, % | 9.9 ± 2.4 | 13.0 ± 2.5 | 15.6 ± 2.4 | 9.5 ± 2.4 | 11.8 ± 1.5 | 13.7 ± 2.5 |

The mechanical properties of CS/CN films prepared from slurry 6 (Table 13) have been improved considerably after modification of the films with PGPR or PLA. The values of the elastic modulus increased six-fold compared with unmodified film. The values of the ultimate tensile stress increased about twice while simultaneously decreasing the strain at break of both modified films.

Strengthening of the films containing mineral substances has also occurred but the values of their elastic modulus and strain at break changed considerably less after modification with PLA and PGPR. In both cases, the increase in the values of contact angles was observed, especially for films modified with PGPR. It should be noted that the adsorption of PLA and PGPR within the plasticized CS/CN films was probably accompanied by the extraction of the molecules of both acetic acid and glycerol from the films into dioxane.

Practically the same changes in mechanical characteristics of CS/CN films containing monolignols and nanolignin occurred after their modification with PLA or PGPR (Table 15).

It is interesting that the order of strengthening of CS/CN films containing ions of the alkali earth metals coincided with the order of increasing their ionic radii equal

to 66 pm, 99 pm and 134 pm for Mg⁺², Ca⁺² and Ba⁺², respectively. The highest and lowest values of the elastic modulus and the ultimate tensile stress have been observed for PGPR- and PLA-modified CS/CN films containing Mg⁺² and Ba⁺² ions. The most strengthened films with Mg⁺² ions have the lowest values of strain at break (Table 16).

Commercial wrapping paper from cellulose used for food packaging and PLA- or PGPR-modified plasticized CS/CN films named CHITOPACK have the comparable values of elastic modulus and ultimate tensile stress (Table 17). However, elasticity of CHITOPACK films are about 3–4 times higher than that of commercial paper such as KFC paper widely used in fast food restaurants for packaging of sandwiches.

Table 17. Comparison of the mechanical characteristics of the commercial films for food packaging with PLA- or PGPR-modified (CS/CN)/pG-3 films with the formulation: (70/30)/25 wt. %.

| Film | Composition | Surface Modifier | Y, MPa | σ , MPa | ϵ , % |
|------|-----------------|------------------|------------|----------------|----------------|
| 1 | CHITOPACK | PGPR | 4792 ± 496 | 81.2 ± 7.5 | 9.7 ± 2.8 |
| 2 | —“—“—“—“— | PLA | 4891 ± 594 | 74.7 ± 5.1 | 7.7 ± 2.2 |
| 3 | Packaging paper | unknown | 4489 ± 136 | 44.8 ± 5.7 | 2.1 ± 0.7 |
| 4 | KFC paper | unknown | 4891 ± 211 | 71.8 ± 6.8 | 2.3 ± 0.3 |
| 5 | DOMOPACK | none | 196 ± 23 | 15.6 ± 1.8 | 623.0 ± 111 |

4. Conclusions

Summarizing the results of the research, it should be concluded that the native linear polysaccharide polymer extracted from crustaceans' carapaces in the form of chitin nanofibrils (CN) has proved to be a potent “physical crosslinker” forming numerous stable noncovalent bonds with chitosan chains by such a way that the CS/CN films do not dissolve in contact with water for a long time without any additional crosslinking.

It was found that there was a limit of saturation of CS phase with CN at about 10 wt. %-content from CS amount in slurry. At higher CN content, the unbound CN were concentrated in the surface-adjacent layer with higher density of packaging components because some chitosan chains present between chitin nanofibrils.

The CS/CN slurries have good compatibility with various low- and high-molecular-weight substances such as ions of the alkali earth metals (Mg, Ca, Ba) and monolignols, nanolignin and gelatin. These substances exhibited some reinforcing effects on the CS chain community. In contrast, the plasticizers disintegrated the interactions between CS and CN in the films. Therefore, their content should be limited by 20–30 wt. %.

The surface modification of CS/CN films by sorption immobilization of PLA or PGPR exhibited great effect on improvement of both mechanical stability and hydrophobicity of CS/CN films. This finding opens the wide avenue for optimizing characteristics of the films in the manner similar to that used by nature in the creation of a polysaccharide-mineral nanocomposite having a hydrophobic layer consisting of hydrocarbon'' molecules on the surface of crustaceans' carapaces.

Chitosan is a very sensitive and malleable polymer, the properties of which are strongly influenced by such factors as temperature, conditions and duration of storage, exposure to light, infrared, ultrasonic or microwave irradiation, intensity of stirring and acidity of its solutions, the microheterogeneity and chemical nature of a support used for casting the CS/CN slurries, the conditions and temperature of their drying, and subsequent hydrophobization of the obtained films. It should be emphasized, that in addition to factors mentioned above, it is extremely important to control the quality of raw materials in order to produce of the CHITOPACK packaging films with reproducible characteristics.

The formed CS/CN composite films seem to be promising candidates for production of completely biodegradable films comparable in their mechanical stability with commercial wrapping paper that is used nowadays for one-off packaging of some food products. Indisputably, the innovative CHITOPACK films will gain an extremely widespread in the future, especially, in the Floating Cities [29] owing to easy biodegradability of the films' components and their bio-compatibility with the Environment.

Author Contributions: Preparation of chitin nanofibrils/chitosan composite films, analysis of the results and coordination of experimental work (Galina Tishchenko); coordination of the research and preparation of chitin nanofibrils (Pierfrancesco Morganti and Marco Stoller); measuring and analysis of mechanical properties of the composite films (Ivan Kelnar and Ludmila Kaprálková); investigation of rheological properties of chitin nanofibrils/chitosan slurries (Jana Mikešová); thermogravimetric analysis and differential scanning calorimetry of the composite films (Jana Kovářová); investigation of the effect of temperature and copper ions on crystallinity of chitin nanofibrils (Jindřich Hašek and Radomír Kužel); determination of molecular weight of chitosans by size-exclusion chromatography (Miloš Netopilík); SEM and TEM of the surfaces and fractures of composite films (Ewa Pavlová); AFM analysis of the morphology of chitin nanofibrils and surfaces of the composite films in the swollen state in water (Eliška Chanová) and in the dry state (Milena Špírková); measuring the sorption of water vapors, gas permeability and contact angles of composite films (Libuše Brožová); FTIR spectroscopy of chitosan nanofibrils, chitosans and composite films (Michal Pekárek); the solid state ¹³C CP/MAS NMR of chitosan nanofibrils, chitosans and composite films (Libor Kobera); synthesis of polylactides (Dana Kubies); surface modification of the composite films by PLA and PGPR (Zdenka Sedláková).

Acknowledgments: We thank the EU for the financial support given to the European Research Projects: n-Chitopack, grant No. 315233 and Biomimetic, grant No. 282945.

Conflicts of Interest: We declare that Galina Tishchenko has no conflict of interest. Pierfrancesco Morganti works in the R&D Centre of Nanoscience, MAVI Sud Srl, Italy.

References

1. Raabe, D.; Al-Sawalmih, A.; Romano, P.; Sachs, C.; Brokmeier, H.G.; Yi, S.-B.; Servos, G.; Hartwig, H.G. Structure and crystallographic texture of arthropod bio-composites. *Mater. Sci. Forum* **2005**, *495–497*, 1665–1674. [CrossRef]
2. Swift, N.B. Biomineral Structure and Strength of Barnacle Exoskeletons. *Colgate Acad. Rev.* **2012**, *8*, 10.
3. Martin, J.W. *Concise Encyclopedia of the Structure of Materials*; Elsevier: Oxford, UK; Amsterdam, The Netherlands, 2007.
4. Morganti, P.; Muzzarelli, C. Production of Nanofibrillar Chitin. U.S. Patent 2008/0118563 A1, 2009.
5. Muzzarelli, R.A.A.; Morganti, P.; Morganti, G.; Palombo, P.; Palombo, M.; Biagini, G.; Belmonte, M.M.; Giantomassi, F.; Orlandi, F.; Muzzarelli, C. Chitin nanofibrils/chitosan glycolate composites as wound medicaments. *Carbohydr. Polym.* **2007**, *70*, 274–284. [CrossRef]
6. Franca, E.F.; Freitas, L.C.G.; Lins, R.D. Chitosan Molecular Structure as a Function of N-Acetylation. *Biopolymers* **2011**, *95*, 448–460. [CrossRef] [PubMed]
7. Yomota, C.; Miyazaki, T.; Okada, S. Determination of the viscometric constants for chitosan and the application of universal calibration procedure in its gel permeation chromatography. *Colloid Polym. Sci.* **1993**, *271*, 76–82. [CrossRef]
8. Netopilík, M.; Bohdanecký, M. Ubbelohde viscometer modified for foaming solutions of water soluble polymers. *Eur. Polym. J.* **1995**, *31*, 289–290. [CrossRef]
9. Morganti, P.; Tishchenko, G.; Palombo, M.; Kelnar, I.; Brozova, L.; Spirkova, M.; Pavlova, E.; Kobera, L.; Carezzi, F. *Marine Biomaterials: Characterization, Isolation and Applications*; Kim, S.-K., Ed.; CRC Press, Taylor & Francis Group: Boca Raton, FL, USA, 2013; pp. 681–716.
10. Ifuku, S.; Shervani, Z.; Saimoto, H. Chitin Nanofibers, Preparations and Applications. In *Nanotechnology and Nanomaterials, Advances in Nanofibers*; Maguire, R., Ed.; InTechOpen: Rijeka, Croatia, 2013; pp. 85–101.
11. Youn, D.K.; No, H.K.; Kim, D.S.; Prinyawiwatkul, W. Decoloration of chitosan by UV irradiation. *Carbohydr. Polym.* **2008**, *73*, 384–389. [CrossRef]
12. Younes, I.; Rinaudo, M. Chitin and Chitosan Preparation from Marine Sources. Structure, Properties and Applications. *Mar. Drugs* **2015**, *13*, 1133–1174. [CrossRef] [PubMed]
13. TA Instruments. Understanding rheology of structured fluids. 2015. Available online: http://www.tainstruments.com/pdf/literature/AAN016_V1_U_StructFluids.pdf (accessed on 1 November 2017).
14. Adamson, A.W.; Gast, A.P. *Physical Chemistry of Surfaces*, 6th ed.; John Wiley & Sons, Inc.: Stanford, CA, USA, 1997.
15. Mikesová, J.; Hasek, J.; Tishchenko, G.; Morganti, P. Rheological study of chitosan acetate solutions containing chitin nanofibrils. *Carbohydr. Polym.* **2014**, *112*, 753–757. [CrossRef] [PubMed]
16. Mistler, R.E.; Twiname, E.R. *Tape Casting. Theory and Practice*; The American Ceramic Society: Westerville, OH, USA, 2000.

17. Ozcelik, B.; Brown, K.D.; Blencowe, A.; Daniell, M.; Stevens, G.W.; Qiao, G.G. Ultrathin chitosan–poly(ethylene glycol) hydrogel films for corneal tissue engineering. *Acta Biomater.* **2009**, *9*, 6594–6605. [CrossRef] [PubMed]
18. Martínez-Camacho, A.P.; Cortez-Rocha, M.O.; Ezquerro-Brauer, J.M.; Graciano-Verdugo, A.Z.; Rodríguez-Félix, F.; Castillo-Ortega, M.M.; Yépiz-Gómez, M.S.; Plascencia-Jatomea, M. Chitosan composite films: Thermal, structural, mechanical and antifungal properties. *Carbohydr. Polym.* **2010**, *82*, 305–315. [CrossRef]
19. Fimbeau, S.; Grelier, S.; Copinet, A.; Coma, V. Novel biodegradable films made from chitosan and poly(lactic acid) with antifungal properties against mycotoxinogen strains. *Carbohydr. Polym.* **2006**, *65*, 185–193.
20. Arvanitoyannis, I.S. Nakayama, A. Aiba Sei-ichi, Chitosan and gelatin based edible films: State diagrams, mechanical and permeation properties. *Carbohydr. Polym.* **1998**, *37*, 371–382. [CrossRef]
21. Bourtoom, T.; Chinnan, M.S. Preparation and properties of rice starch–chitosan blend biodegradable film. *LWT Food Sci. Technol.* **2008**, *41*, 1633–1641. [CrossRef]
22. Fernandes, S.C.M.; Freire, C.S.R.; Silvestre, A.J.D.; Neto, C.P.; Gandini, A.; Berglund, L.A.; Salmén, L. Transparent chitosan films reinforced with a high content of nanofibrillated cellulose. *Carbohydr. Polym.* **2010**, *81*, 394–401. [CrossRef]
23. Bhatt, A.S.; Bhat, D.K.; Santosh, M.S. Electrochemical properties of chitosan–Co₃O₄ nanocomposite films. *J. Electroanal. Chem.* **2011**, *657*, 135–143. [CrossRef]
24. Leceta, I.; Guerrero, P.; de la Caba, K. Functional properties of chitosan-based films. *Carbohydr. Polym.* **2013**, *93*, 339–346. [CrossRef] [PubMed]
25. Huang, D.; Mu, B.; Wang, A. Preparation and properties of chitosan/poly(vinyl alcohol) nanocomposite films reinforced with rod-like sepiolite. *Mater. Lett.* **2012**, *86*, 69–72. [CrossRef]
26. Kelnar, I.; Kovářová, J.; Tishchenko, G.; Kaprálková, L.; Pavlová, E.; Carezzi, F.; Morganti, P. Chitosan/Chitin nanowhiskers composites: Effect of plasticisers on the mechanical behaviour. *J. Polym. Res.* **2015**, *22*, 1–6. [CrossRef]
27. Stern, S.A. The “Barrer” Permeability Unit. *J. Polym. Sci.* **1968**, *6*, 1933–1934. [CrossRef]
28. Pauly, S. Permeability and Diffusion Data. In *Polymer Handbook*; Brandrup, J., Immergut, E.H., Grulke, E.A., Eds.; John Wiley and Sons: New York, NY, USA, 1999; pp. 435–446.
29. World’s first floating city to be built off the coast of French Polynesia by 2020. Available online: www.independent.co.uk/news/science/floating-city-french-polynesia-2020-coast-islands-south-pacific-ocean-peter-thiel-seasteading-a8053836.html (accessed on 6 November 2018).